To the Graduate Council:

I am submitting herewith a thesis written by Peter Angelini entitled "Part I. Determination of the Melting Point and Phase Transformation Temperatures of Promethium-147 Metal and Part II. Vapor Pressure of Curium-244 Metal." I recommend that it be accepted in partial fulfillment of the requirements for the degree of Master of Science, with a major in Physics.

Paul G. Huray

Paul Huray, Major Professor

We have read this thesis
and recommend its acceptance:

John O Thomson

Joseph R Peterson

Accepted for the Council:

Hilton A Smith

Vice Chancellor
Graduate Studies and Research

ℓ

PART I. DETERMINATION OF THE MELTING POINT AND PHASE TRANSFORMATION TEMPERATURES OF PROMETHIUM-147 METAL

PART II. VAPOR PRESSURE OF CURIUM-244 METAL

A Thesis

Presented for the

Master of Science

Degree

The University of Tennessee

Peter Angelini

June 1974

ACKNOWLEDGMENTS

The author wishes to express his appreciation to the Oak Ridge National Laboratory* for the use of the equipment in the experiment. In addition, the author would like to thank the following people: R. E. McHenry of Oak Ridge National Laboratory for his interest and direction in the experiments; Dr. P. G. Huray of the University of Tennessee who served as faculty advisor; H. L. Adair of the Oak Ridge National Laboratory for preparing the metal samples; T. R. Rice of Oak Ridge National Laboratory for his assistance in the performance of the promethium experiment; T. D. Owings of Oak Ridge National Laboratory for his assistance in the performance of the curium experiment; and S. K. Whatley of Oak Ridge National Laboratory for typing the manuscript.

Finally, the author is grateful to his wife Suzanne for her encouragement and help in the completion of the manuscript.

*Research sponsored by the United States Atomic Energy Commission under contract with the Union Carbide Corporation.

1146826

ABSTRACT

The promethium metal used in the determination of the melting point and phase transition temperatures had been prepared by reduction of promethium oxide with thorium metal at 1300°C and volatilization of promethium metal at 1600°C. The melting point and phase transformation temperatures of promethium metal were found to be 1042 ± 3°C and 890 ± 5°C, respectively. The Debye temperature was estimated to be 1042 ± 13°K, and the ratio for the heat of the high-temperature transformation to the heat of fusion was determined to be 0.415.

The vapor pressure of liquid and solid ^{244}Cm metal between 1270 and 1905°K was measured by the Knudsen effusion method to be

$$\log_{10}[P(atm)] = (3.85 \pm 0.41) - [(17{,}915 \pm 640)/T°K] \ .$$

The $\Delta H_{1600°K}$ and $\Delta S_{1600°K}$ for vaporization are 82.0 ± 2.9 kcal/mole and 17.5 ± 1.9 e.u., respectively. An x-ray diffraction analysis of the initial ^{244}Cm metal indicated a f.c.c. structure with a 5.033 ± 0.003 Å lattice parameter.

TABLE OF CONTENTS

SECTION PAGE

PART I. DETERMINATION OF THE MELTING POINT AND PHASE TRANSFORMATION TEMPERATURES OF PROMETHIUM-147 METAL

INTRODUCTION 2

I. MATERIAL 4

Preparation of Promethium-147 Metal
Purity of Promethium-147 Metal
Melting Point Standards

II. APPARATUS 6

Glove Box
High-Temperature Vacuum Furnace
Pyrometer
Instruments

III. PROCEDURE 10

Method of Melting Point Measurement
MgO Crucible Method
Modified MgO Crucible Method
W5Re-W26Re Differential Thermocouple Method
Pt-Pt10Rh Thermocouple Method

IV. RESULTS 17

MgO Crucible Method
Modified MgO Crucible Method
W5Re-W26Re Differential Thermocouple Method
Pt-Pt10Rh Thermocouple Method

V. DISCUSSION 24

Promethium Melting Point Temperature
Debye Temperature
Solid-Solid Phase Transformation

SECTION PAGE

PART II. VAPOR PRESSURE OF CURIUM-244 METAL

INTRODUCTION 34

VI. THEORY 35

VII. MATERIAL 40

Initial Cm_2O_3 Material

VIII. APPARATUS 42

Vapor Pressure Determination Apparatus
X-Ray Diffraction Unit
Knudsen Cell

IX. PROCEDURE 46

Curium Metal Sample Loading
Temperature Measurement
Sample Collection and Measurement
X-Ray Diffraction

X. RESULTS 48

Pyrometer Calibration
X-Ray Diffraction
Vapor Pressure

XI. DISCUSSION 53

LIST OF REFERENCES 56

VITA 60

LIST OF TABLES

TABLE		PAGE
1.	Spark Source Mass Spectrometric Analysis of the Resulting Promethium-147 Metal	5
2.	Modified MgO Crucible Calibration Results	17
3.	Modified MgO Crucible Promethium Metal Melting Point Results	18
4.	W5Re-W26Re Gold Melting Point Calibration	19
5.	W5Re-W26Re Promethium Melting Point and Phase Transition Temperature Results	22
6.	Debye Temperature Data	27
7.	Heat of Fusion and Heat of High-Temperature Phase Transformation for the Rare-Earth Metals	29
8.	Silver and Gold Melting Point Area Determinations	31
9.	Curium Isotopic Content	40
10.	Impurities in Batch SRL-31 Curium Oxide	40
11.	Optical Pyrometer Calibration	48
12.	X-Ray Diffraction Results of ^{244}Cm Metal	49
13.	Vapor Pressure Data	50
14.	Coefficients of Fitted Equation	51
15.	Statistical Analysis of Vapor Pressure Data	51

LIST OF FIGURES

FIGURE		PAGE
1.	Argon Atmosphere Glove Box	6
2.	High-Temperature Vacuum Furnace	8
3.	MgO Crucible Assembly	11
4.	W5Re-W26Re Differential Thermocouple Assembly	14
5.	Thermograph of a Gold Melting Point Experiment	19
6.	Promethium Metal Thermograph on the Sample's Second Melt	20
7.	Promethium Metal Thermograph of the High-Temperature Phase Transition	21
8.	Melting Point and High-Temperature Phase Transformation Data for the Rare-Earth Metals	28
9.	Vapor Pressure Collection Assembly	42
10.	Furnace Heat Zone	45
11.	Vapor Pressure of Curium-244 Metal	52

PART I. DETERMINATION OF THE MELTING POINT AND PHASE TRANSFORMATION TEMPERATURES OF PROMETHIUM-147 METAL

INTRODUCTION

The object of this experiment was to determine the melting point of promethium metal. Various values for the melting point had been reported ranging from 865 to 1168°C. Promethium metal has been prepared by Weigel (1) on a milligram scale by reduction of PmF_3 with lithium in a tantalum crucible system. The melting point reported for promethium metal was 1080 ± 10°C. In additional work, the melting point was later revised by Weigel (2) to be 865 ± 40°C.

Wheelwright (3) has also reported the preparation of kilogram quantities of promethium metal. In this case, the promethium was prepared by calcium reduction of anhydrous $PmCl_3$. Additional purification was obtained by vacuum distillation of calcium and magnesium impurities. The melting point of promethium metal was reported by Wheelwright (3) to be 1168 ± 6°C.

In the present paper the determination of the melting point and phase transformation temperatures of promethium metal are reported to be 1042 ± 5°C and 890 ± 5°C, respectively.

The Lindemann (4) melting formula was used to calculate the Debye temperature of promethium metal.

$$\theta_D = c'\sqrt{T_m}/\sqrt{A}(w)^{1/3} \qquad (1)$$

where

θ_D = Debye temperature,
T_m = melting point temperature,
A = atomic weight,
w = atomic volume, and
c' = constant.

The function is not strongly sensitive in temperature. When one substitutes values of T_m, θ_D, A, and w in equation (1) and solves for the constant c´, one obtains values of c´ which are nearly equal for elements of similar electronic and structural characteristics. Thus it can be used to estimate the Debye temperature of an element after one obtains a value for c´ calculated for an element of similar characteristics.

The Lindemann (5) melting formula is based on the idea that a substance will melt when the root-mean-square displacement of each atom in a solid becomes a certain fraction of the mean radius of the unit cell. The mean-square amplitude of vibration of an atom about its lattice site is given by

$$D = 9\hbar^2 T/Ak\theta^2 \qquad (2)$$

where

$\hbar$ = Planck's constant/2π

k = Boltzmann's constant,

θ = Debye temperature,

A = atomic weight, and

T = temperature.

If melting is assumed to occur when the mean-square displacement of atoms becomes a certain fraction, x_m, of the unit cell distance, r_s, then the melting point temperature, T_m, can be related to atomic constants.

$$T_m = (x_m^2/9\hbar^2)Ak\theta^2 r_s^2 \qquad (3)$$

I. MATERIAL

Preparation of Promethium-147 Metal

The preparation of the ^{147}Pm metal sample was previously described in an article by Angelini and Adair (6). A summary of the preparation technique will be given here. The reduction–distillation process was used to obtain the promethium metal. The process was performed in a vacuum furnace contained in an argon atmosphere glove box. Promethium-147 oxide was mixed with 5% stoichiometric excess of thorium metal powder. Cold-pressed pellets were made of the mixture, and the pellets were loaded into a tantalum metal reaction crucible. The reaction crucible was placed in a vacuum furnace and the temperature taken to 1300°C. Samarium, the product from the nuclear decay of ^{147}Pm in the reaction $^{147}Pm \xrightarrow{\beta^-} {}^{147}Sm$, was distilled at this temperature as the metal and collected on a quartz dome. After it had been determined from weight loss measurements that all of the samarium metal had been distilled, the reaction crucible was placed in the vacuum furnace and the temperature taken to 1600°C. The promethium metal was distilled at this temperature and was collected onto a quartz dome.

Purity of Promethium-147 Metal

Approximately 10 mg of promethium metal was sent for spark-source mass spectrometric analysis to the Mass and Emission Spectrometry Section of the Analytical Chemistry Division of Oak Ridge National Laboratory. The results of the analysis are presented in Table 1. The concentration of tantalum in the final ^{147}Pm metal product was <1 wt (ppm). The concentration of thorium metal in the product was ~10 wt (ppm). Thus, there

occurred little sublimation of tantalum or thorium metal during the promethium distillation process. There also occurred little if any vaporization of other lanthanides. The low concentration of samarium in the product indicated that the vast majority of the samarium had been reduced and vaporized during the samarium distillation procedure. The analysis indicated that very pure promethium metal may be obtained by the reduction–distillation process.

Table 1. Spark Source Mass Spectrometric Analysis of the Resulting Promethium-147 Metal

Element	Weight (ppm)	Element	Weight (ppm)
Al	10	S	0.3
Ba	0.2	Sc	<1
Ca	200	Y	<1
Co	<0.1	La	<1
Cr	7	Ce	<1
Cu	4	Pr	<1
Fe	100	Nd	20
K	20	Sm	2
Mn	0.7	Eu	<1
Ni	4	Gd	<1
P	<0.1	Tb	<1
Pb	50	Dy	<1
Li	20	Ho	<1
Ta	0.7	Er	<1
Th	9	Tm	<1
Ti	<0.2	Yb	<1
V	<0.1	Lu	<1
Zn	3	Pm	Major
Cl	700		

Melting Point Standards

The silver and gold reference materials used for melting point calibration experiments were NBS Standard Reference Material 748 and 745, respectively.

II. APPARATUS

Glove Box

The promethium metal was transferred to an argon atmosphere glove box capable of handling radioactive materials such as ^{147}Pm (see Figure 1). The glove box was a modified high-level, alpha-handling, hot cell. The front of the hot cell served as the main access area. The front access plate contained a plate glass viewing window having four glove ports, a 14-in. bag-in and bag-out entry port, two vacuum line feedthroughs, three electrical feedthroughs, eight BNC-type-connector on coaxial cable (BNC cable) feedthroughs, and two filtered gas inlet lines. An additional access area was located on the top of the glove box. The top access area contained a plate glass viewing window having two glove ports.

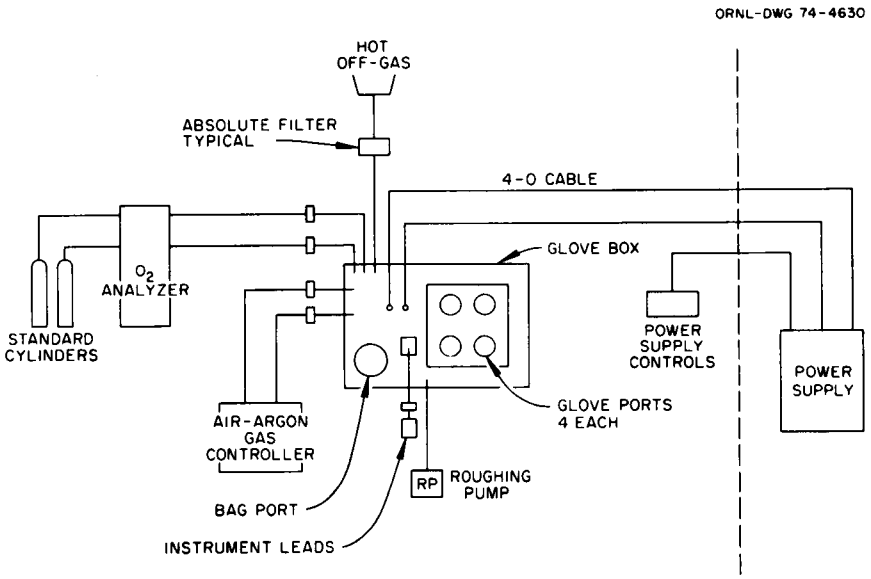


Figure 1. Argon Atmosphere Glove Box.

Two other glove-box-associated instruments were the gas inlet manifold, which automatically controls the glove box negative pressure, and a Beckman G2 oxygen analyzer. Two standardized compressed gases were used to calibrate the oxygen analyzer. These were a pure argon gas and a 700-ppm oxygen remainder argon-compressed gas cylinders.

High-Temperature Vacuum Furnace

The high-temperature vacuum furnace used was designed by various Isotopes Division personnel and fabricated by personnel of the Plant and Equipment Division at ORNL. Figure 2 is a diagram of the furnace. The octal base ports permit access within the furnace. On these ports were located a main vacuum line, a thermocouple vacuum gage, an ionization gage, a backfill valve, and an octal instrument with the remainder of the ports sealed with blank flanges. Viton O-ring seals were used on all vacuum ports.

The furnace bonnet, the base plate, the bonnet access unit, the power posts, and the main power leads were water-cooled by means of a closed-loop recirculating chilled-water supply. The bonnet and base plate were made of aluminum metal. The water-cooled power posts were made of copper. The heat shields were made from five sheets of 20-mil molybdenum metal, and the heating element was made from 15-mil tantalum metal.

The heating element was of the double-spiral type and was 1-1/2-in. wide and 4-in. long. The interior of the heat zone could be seen through a 1/4-in. hole punched in the heating element and through a 1/2-in. hole in the molybdenum heat shield. The furnace could obtain a maximum temperature of 2100°C in a two-minute period from an ambient condition.

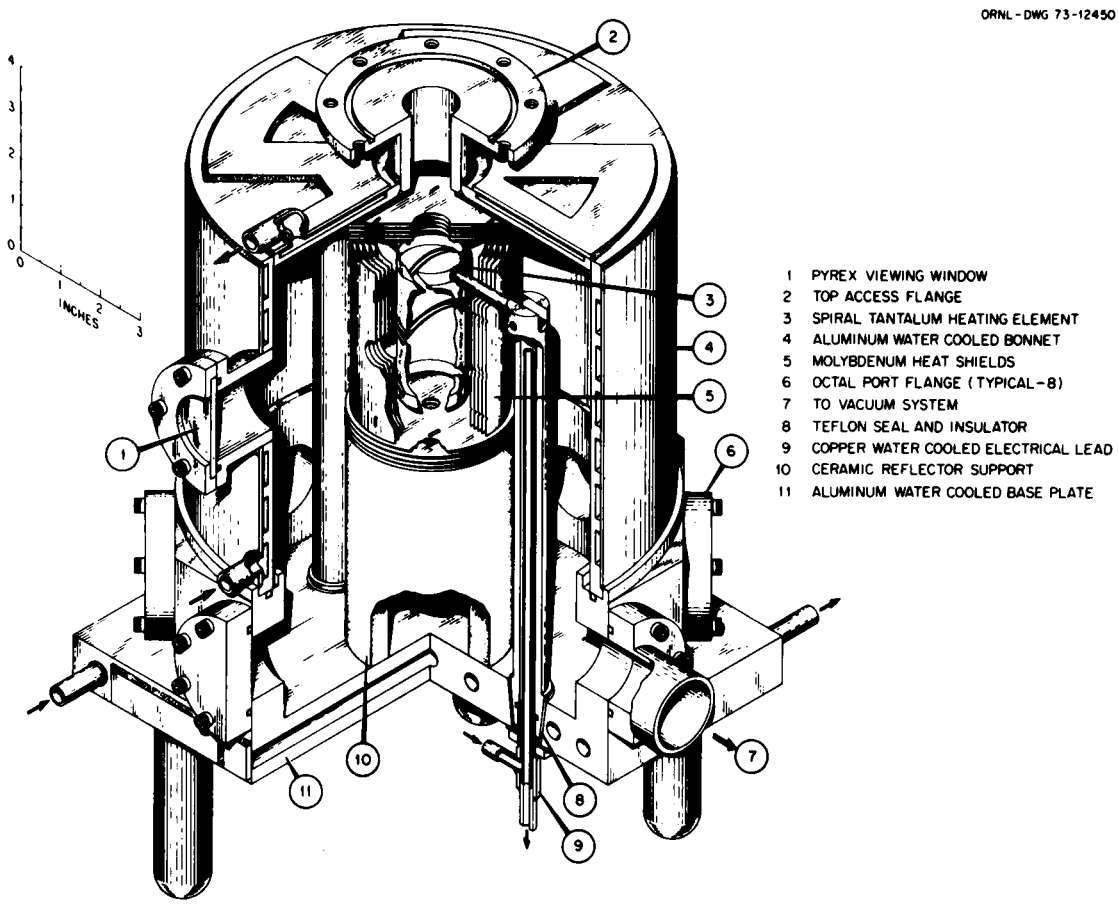


Figure 2. High-Temperature Vacuum Furnace.

The furnace DC power supply was a modified 600-amp welder. The unit was located in a separate room, and power was transmitted to the furnace by two 4-0 flexible copper cables. The output power could be ramped either up or down and held at prescribed power levels. The controls for ramping the supply, the safety on-off switch, and the output current and voltage meters were located in the operating area near the glove box.

The furnace vacuum system included a Welch 2.1-cfm mechanical roughing pump, an air-cooled 2-in. Varian oil diffusion pump, a water-cooled oil vapor baffle, and an absolute filter. The mechanical pump and absolute filter were located outside the glove box, and the diffusion pump

and baffle were in the glove box. A flexible vacuum line was used to connect the two vacuum pumps.

The experimental equipment was safety interlocked. A furnace thermocouple vacuum gage and set point controller would turn off both the furnace cooling water supply and the furnace power supply if the pressure increased above the set point. A fire alarm probe on the glove box would alarm and turn off all power and water to the furnace if a heated condition existed. A water-pressure switch on the furnace outlet water line would turn off both the furnace water supply and the furnace power supply if the outlet water pressure decreased below a set value. The system would have to be manually reset if a failure condition had shut down the equipment.

Pyrometer

A pyrometer was used to measure temperature and observe the sample area. The unit, Model No. 95 fabricated by The Pyrometer Instrument Company, was of the brightness measuring, disappearing filament type.

Instruments

Various instruments were used to measure the output of the thermocouples. These were a Tektronik Model 5031 dual beam storage oscilloscope, a Keithly Model 151 nullmeter microvoltmeter, a Hewlett Packard Model 3440-A digital voltmeter with 3444-ADC multifunction unit, and a constant voltage supply. The instruments had been calibrated prior to use.

III. PROCEDURE

Method of Melting Point Measurement

MgO Crucible Method

The rare-earth elements are very reactive when in the metallic form. The rare-earth oxides are some of the most stable oxides known (7). The metals also alloy very easily and form solid solutions, eutectics, and compounds with each other and nearly every other element (8). Such processes occur at ambient temperatures and pressures, but also to a greater extent at high temperature. A material with which promethium metal would not react or with which a minimum of reaction would occur needed to be found in order to obtain a meaningful melting point temperature. Magnesium oxide (MgO) was chosen as the container material (9) for promethium metal. The free energy of formation of MgO is more negative than that of Pm_2O_3 to temperatures greater than 1200°C. Thus, thermodynamically speaking, promethium metal should not react with MgO. Above 1200°C, MgO is quite volatile in vacuum; however, the maximum temperature at which the sample and crucible would be in contact was not expected to exceed 1200°C. Other oxides more stable than MgO exist; however, their fabrication qualities are not as good as those of MgO. Thus, MgO crucibles were fabricated and an assembly as shown in Figure 3 was made. The unit used one Pt—Pt10Rh thermocouple with the thermocouple junction being in a hole drilled into the bottom of the MgO crucible.

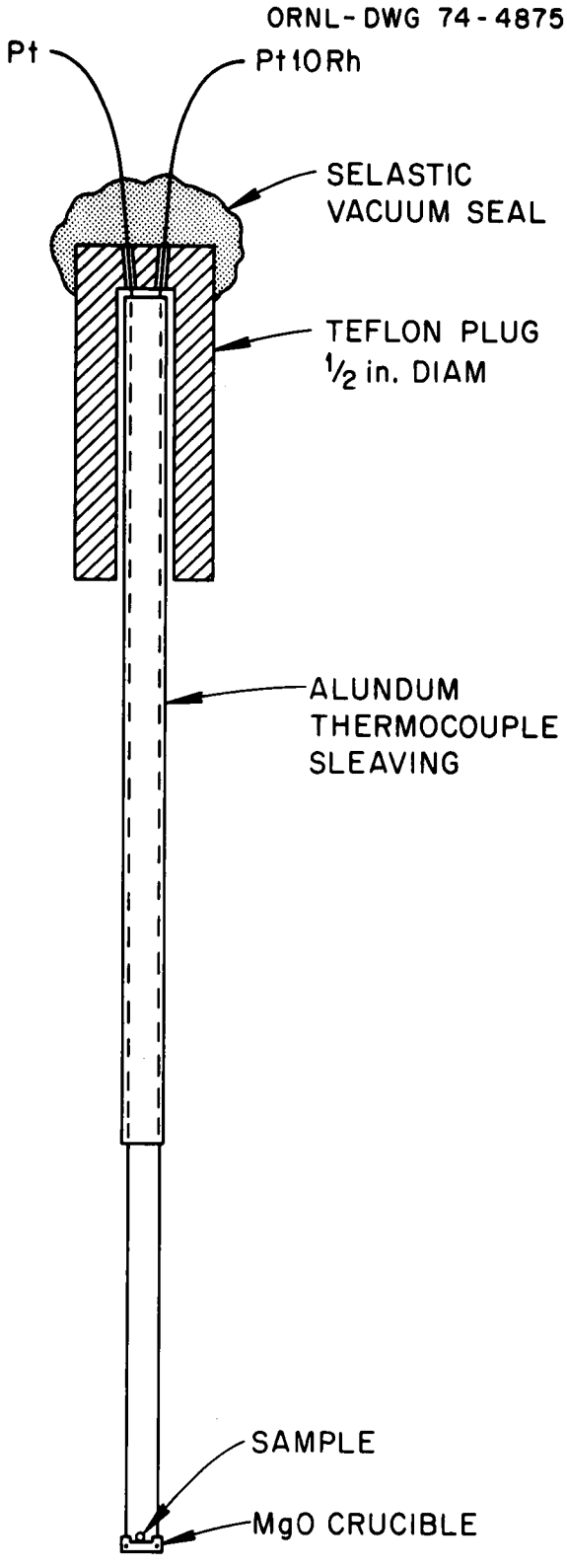


Figure 3. MgO Crucible Assembly.

During an experiment ∿70 mg of promethium metal was placed in the MgO crucible and the thermocouple assembly placed in the furnace. Insulated copper wire with clips was used to connect the thermocouple wires to the BNC cables. On the outside of the glove box the same type of insulated copper wire was used to connect the signal leads of the BNC cable to the measuring instrument. The data obtained in using silver and gold as melting point temperature standards were used for calibrating the promethium metal data. Corrected temperature readings were then obtained by linearly interpolating these data. This same type of wiring procedure was used in the modified MgO crucible method described below. The sample temperature was then increased and equilibrated at 900°C. At this level, the furnace temperature was ramped at a rate of 20°C/min until the melting point was indicated in the electromotive force (EMF) output of the thermocouple. The sample which was located in the center of the heat zone was observed with the pyrometer during the temperature increase.

Modified MgO Crucible Method

In this method the MgO crucible was made much smaller, and a second Pt—Pt10Rh thermocouple was placed alongside the crucible but not in contact with it. The walls of the MgO crucible were made smaller such that a sample placed in it could be observed with a pyrometer. Calibration experiments using gold and silver were performed. During these experiments it was determined that both thermocouples produced the same output within experimental error at an equilibrated temperature or during a temperature ramp of 20°C/min. During an experiment the sample was

observed by using the optical pyrometer. The output of one of the thermocouples was recorded to be the melting point when the sample was seen to melt. In each case, upon the first melt the irregular-shaped metal pieces became spherical. During successive melts and freezes there was a distinctive change in the appearance of the metal's surface. The measurement for promethium metal was obtained using the same procedure as with gold and silver. The silver and gold data were linearly interpolated in order to obtain a corrected temperature for promethium.

W5Re-W26Re Differential Thermocouple Method

Another method used to identify not only the melting point but also a high-temperature phase transition of promethium metal was one of differential thermal analysis. The thermocouple assembly is shown in Figure 4. The assembly was fabricated in the same manner as the others mentioned previously. Three thermocouples were used in this unit. The two W5Re-W26Re thermocouples used calibrated wire 10 mils in diameter and were connected such that they formed a difference thermocouple. One of the thermocouples forming the difference thermocouple was fabricated such that the thermocouple bead region was demountable. The thermocouple wire used in the demountable W5Re-W26Re thermocouple section came from the same calibrated roll of wire as the material used in the stationary W5Re-W26Re thermocouple. The demountable thermocouple was necessary so that more than one experiment could be performed with the assembly. The third thermocouple was made from 10-mil Pt-Pt10Rh wire with the thermocouple bead located near the difference thermocouple. The Pt-Pt10Rh thermocouple was the temperature measuring thermocouple. Inside the glove box the thermocouples were connected to the leads of the BNC cables

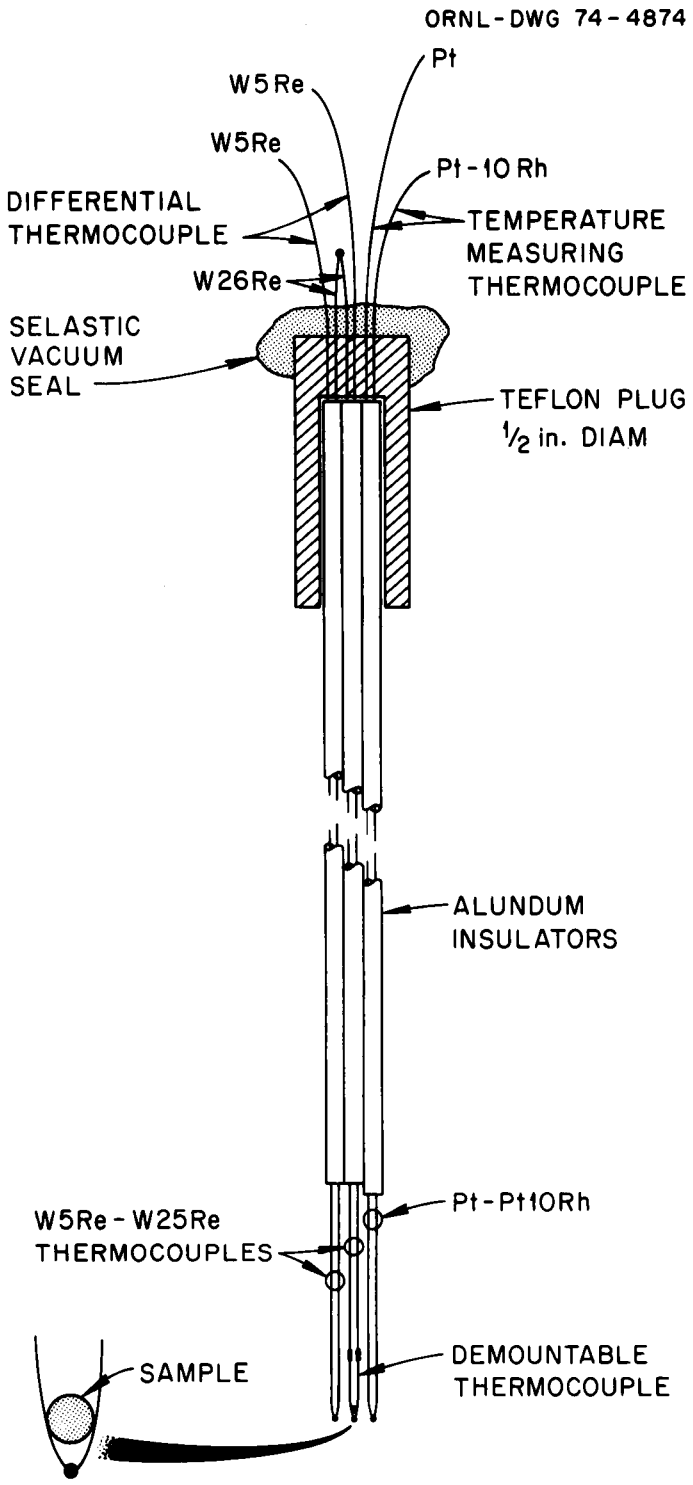


Figure 4. W5Re-W26Re Differential Thermocouple Assembly.

by using the insulated copper wire cables. Outside the glove box the insulated copper cables were used to connect the BNC cable leads of the difference thermocouple directly to the oscilloscope. The output of the Pt-Pt10Rh thermocouple was connected to a 0°C reference junction prior to wiring the signal to the digital voltmeter.

Calibration of the unit was performed by melting gold standards. A small piece of metal was placed on the demountable W5Re-W26Re thermocouple and the assembly loaded into the furnace. The output of the difference thermocouple was recorded on the oscilloscope as a function of time. The temperature of the metal sample was increased and equilibrated at a value below its melting point. The temperature was then ramped at ∿10°C per minute through the melting point of the sample. The output of the Pt-Pt10Rh temperature-measuring thermocouple was recorded to be the melting point when the melting began to affect the output of the difference thermocouple.

In the promethium experiments the glove box was first placed under an inert argon atmosphere. After the oxygen level reached a level of less than 500 ppm, promethium metal was removed from its closed container and the container again closed. The promethium sample was then lodged in the demountable W5Re-W26Re thermocouple and the assembly placed in the vacuum furnace. During the experiment the sample and thermocouple zone of the assembly was observed through the viewing port of the furnace by using an optical pyrometer.

Pt-Pt10Rh Thermocouple Method

Another assembly was fabricated having one Pt-Pt10Rh thermocouple. The unit was fabricated in a similar manner to the others previously

mentioned. The thermocouple wire was from the same roll as the wire used in the other assemblies. In this experiment a sample of promethium metal was lodged in the thermocouple bead area (10). The output of the thermocouple was connected to a 0°C reference junction prior to wiring the signal to the first input of the differential amplifier on the oscilloscope. A constant voltage supply was connected to the second input of the differential amplifier. The constant voltage supply was used to null the output of the thermocouple such that the oscilloscope could be operated at a more sensitive range. During the initial experiment with a promethium sample, the Pt-Pt10Rh thermocouple was observed to react with the promethium metal.

IV. RESULTS

MgO Crucible Method

Approximately 70 mg of promethium metal was placed in the MgO crucible and the unit loaded in the furnace. No EMF change was measured in a temperature range where the promethium metal was observed to melt. Thus, the diffusivity of the MgO container in conjunction with the heat of fusion and the amount of promethium sample prevented the success of this method.

Modified MgO Crucible Method

The results for the silver and gold calibration experiments are presented in Table 2.

Table 2. Modified MgO Crucible Calibration Results

Sample	Observed		Standard	Observed-Standard	
	EMF (mv)	Melting Point (°C)	Melting Point (°C)	EMF (mv)	Temperature (°C)
Ag	9.41	989	961	0.29	28
Ag	9.44	986	961	0.32	25
Au	10.64	1092	1063	0.33	29
Au	10.57	1085	1063	0.26	22

The data reported in Table 2 are on four samples of melting point standards. The samples were each melted and frozen a number of times. In each case, the observed EMF varied only ±0.02 mv.

Two promethium metal samples were used with two melting and freezing experiments performed on each sample. In each case the temperature was taken to 950°C and the system equilibrated. The temperature was then ramped at 20°C/min to above the melting point. After the sample had melted, the temperature was decreased at 20°C/min and the freezing point was measured. No measurable difference between the freezing and melting point was observed.

The results of the promethium metal experiments are presented in Table 3.

Table 3. Modified MgO Crucible Promethium Metal Melting Point Results

Sample	Observed EMF (mv)	Corrected Melting Point (°C)
Pm-1	10.25	1037
	10.23	1035
Pm-2	10.26	1037
	10.29	1039

An additional promethium metal sample was unloaded from its closed container while the glove box was under an inert atmosphere. The remainder of the samples were re-encapsulated. The glove box atmosphere was then replaced with air and the promethium sample exposed to this condition for ∿18 hr. The sample was then placed in the MgO container and a melting point experiment performed. The melting point was measured to occur at 1063°C. This number is significantly higher than the

previous melting points measured using pure promethium metal. This indicates that oxidation of promethium metal will result in higher melting points than those of nonoxidized metal samples (11).

W5Re-W26Re Differential Thermocouple Method

In these experiments the thermographs were recorded as EMF versus time. Figure 5 is a typical thermograph of a gold melting point experiment. Table 4 presents the numerical data associated with the thermograph.

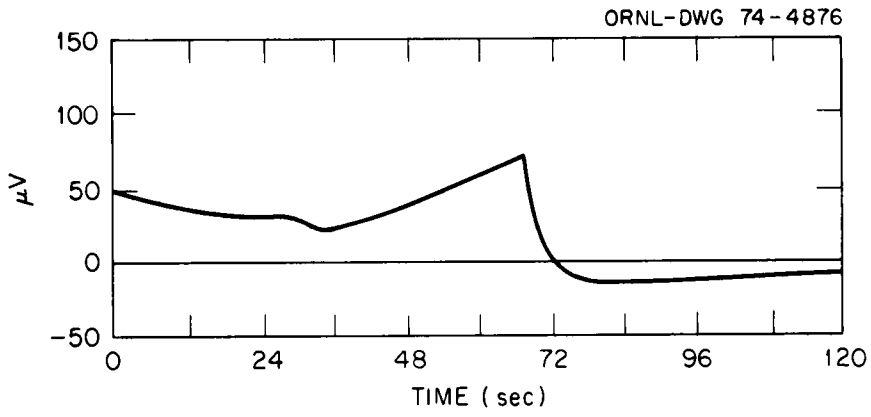


Figure 5. Thermograph of a Gold Melting Point Experiment.

Table 4. W5Re-W26Re Gold Melting Point Calibration

Sample	Gold
Beginning of Melt EMF (mv)	10.23
End of Melt EMF (mv)	10.51
Observed Melting Point (°C)	1057
Standard Melting Point (°C)	1063
Observed-Standard EMF (mv)	-0.07
Observed-Standard Temperature (°C)	-6

The freeze occurred within experimental error of the melt in the gold melting point experiment. Also the measurements did not change in performing the melt and freeze up to four times. The sample was evaporating at a significant rate at these temperatures. This was observed by noting the condensate on the furnace viewing window.

In the promethium metal experiment ∿10 mg of sample was lodged in the demountable thermocouple. Both melting and freezing thermographs were obtained. After the initial melt, the promethium sample had become spherical and completely surrounded the thermocouple bead. The later thermographs were much sharper than the initial one due to better thermal contact between the thermocouple bead and the promethium metal sample. Figure 6 presents one of the promethium metal thermographs on the sample's second melt.

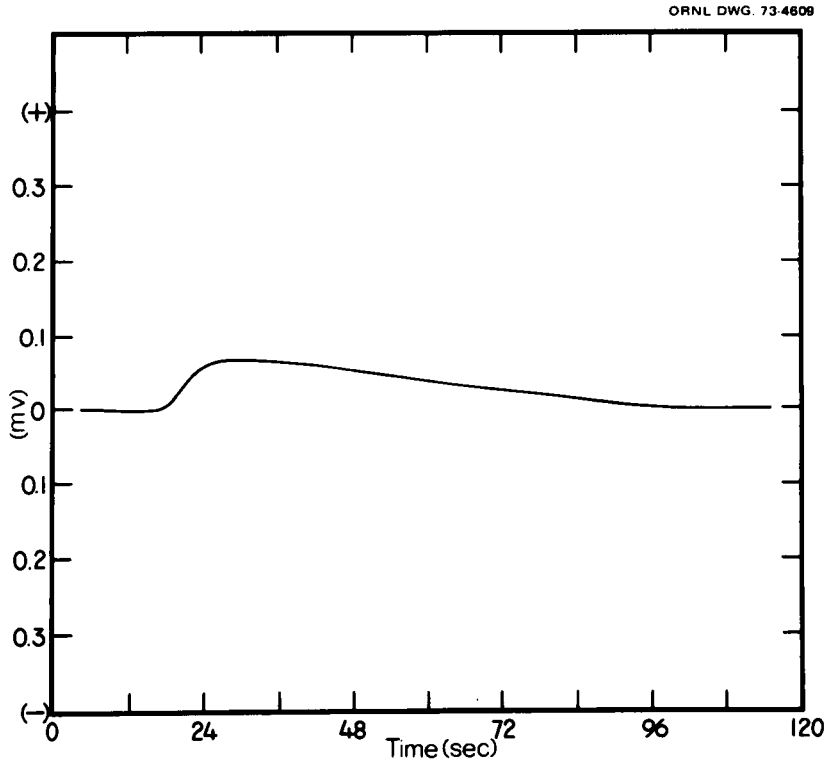


Figure 6. Promethium Metal Thermograph on the Sample's Second Melt.

A second transition was observed to occur at a lower temperature than the melting point. A thermograph of the higher temperature phase transition upon heating is presented in Figure 7. This figure can be directly related to Figure 6, for it was obtained immediately prior to the melt shown in Figure 7.

The temperature at which the high-temperature phase transition occurred did not vary with the number of times it was measured or with the number of melts the sample had undergone. Also no difference in the transition temperature was observed when the temperature was increasing or decreasing through the phase transition temperature.

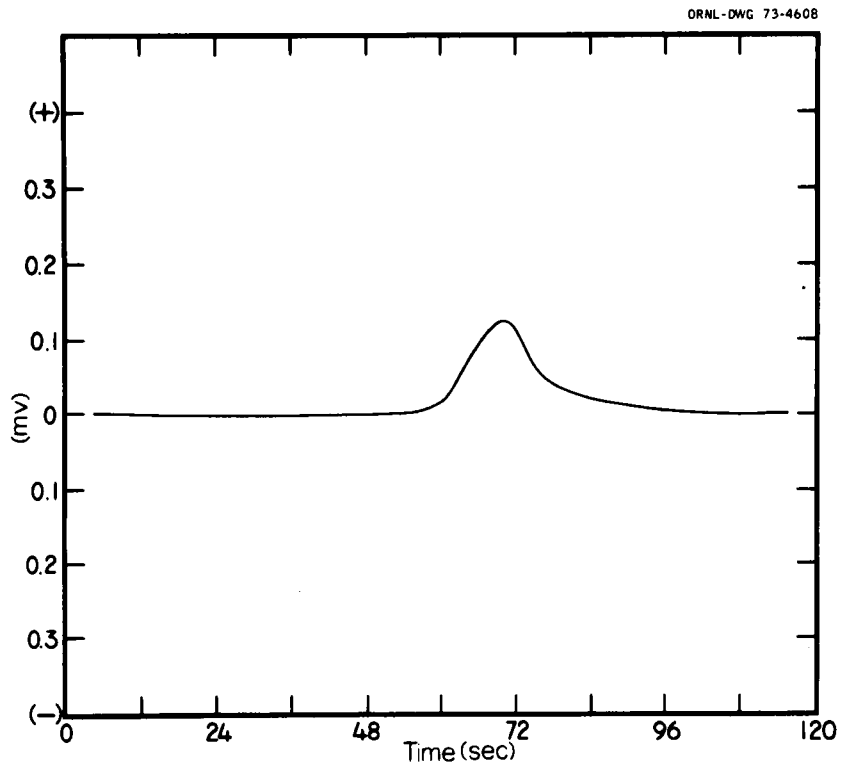


Figure 7. Promethium Metal Thermograph of the High-Temperature Phase Transition.

The numerical data for the melting point and phase transition temperature experiments are presented in Table 5. The corrections obtained from the gold calibration experiment have been applied to the temperature values.

Table 5. W5Re-W26Re Promethium Melting Point and Phase Transition Temperature Results

Phase Transition	Melting Point	Observed EMF (mv)	Corrected Temperature (°C)
T↓		8.25	890
T↑		8.25	890
	T↓	10.06	1048
T↓		8.25	890
T↑		8.25	890
	T↑	10.09	1051
	T↓	10.01	1044
	T↑	10.04	1046
	T↓	9.99	1042

Pt-Pt10Rh Thermocouple Method

In this method a promethium metal sample was lodged on the thermocouple bead. The transition was clearly evident and the temperature at which it commenced was measured to be 893°C. The signal from the thermocouple became increasingly noisy as the temperature was increased. At the temperature at which the promethium metal should have melted, the

peak-to-peak noise level had increased from its ambient temperature value of 30 μV to a value of 3 V peak-to-peak. The melt was completely obscured. Immediately above this temperature range the thermocouple separated; the promethium metal had reacted with the Pt-Pt10Rh thermocouple. Using the thermocouple noise level as an indication of extent of interaction, the reaction was first observed at a temperature slightly lower than the phase transition temperature.

V. DISCUSSION

Promethium Melting Point Temperature

Four determinations of the melting point for ^{147}Pm metal were performed using the modified MgO crucible method. Assigning an accuracy of ±5°C to each temperature measurement, the average melting point temperature within a 95% confidence limit is 1037 ± 2.5°C.

In the W5Re-W26Re differential thermocouple method, five melting point determinations were performed. Assigning an accuracy of ±5°C to each temperature measurement, the average melting point temperature within a 95% confidence limit is 1046 ± 2.2°C.

The average melting point temperature as determined by one method does not fall within the 95% confidence band of the other method. There is a possibility that the two techniques yield different results. This difference, however, was not definitely determined through experimentation with additional samples. Thus equal weight was given to each temperature measurement irrespective of method. Using all of the results for two methods, the average melting point temperature for ^{147}Pm metal is 1042 ± 3°C.

Promethium melting point determinations have been performed by other workers. Promethium metal has been prepared by Weigel (1) on a milligram scale by reduction of PmF_3 with lithium in a tantalum crucible system. The melting point reported was 1080 ± 10°C. Wheelwright (3) has also reported the preparation of gram quantities of promethium metal. In that case, the promethium metal was prepared by calcium reduction of anhydrous $PmCl_3$. Additional purification was obtained by vacuum

distillation of the calcium and magnesium impurities. The melting point of promethium metal was reported by Wheelwright (3) to be 1168 ± 6°C. The method used in obtaining the 1168°C value was to drill a hole in promethium metal and load the material into a furnace. The temperature was then increased and held at a set temperature for a specified time. The furnace was then cooled, the material removed, and the hole observed. The closure of the hole would indicate the melting point temperature. It was noted that partial oxidation of the sample had prevented closure of the hole. As determined in the present work, oxidation of the sample will cause an increase in the melting point for promethium metal. The results of Weigel (1) of 1080°C and Wheelwright (3) of 1168°C for the melting point of promethium metal may have been caused by the partial oxidation of the promethium metal sample. In later experiments Weigel (2) revised the melting point of promethium metal from 1080 ± 10°C to 865 ± 40°C. The latter temperature was obtained by using McWhan's "solder rupture" method. This latter temperature is in the range of the high-temperature phase transition temperature of 890°C as determined by differential thermocouple methods used in the present study. Perhaps the bead in Weigel's (2) latter result ruptured at this polymorphic phase transition temperature. Also various intermetallic compounds exist between the precious metals and the rare-earth metals (12-14). It is evident that such an intermetallic interaction occurred between promethium metal and the Pt-Pt10Rh thermocouples when the metals came in direct contact. This occurred in the Pt-Pt10Rh thermocouple method of of the present work and in the thermocouple arrest method used unsuccessfully by Wheelwright.(3)

Debye Temperature

One may use the Lindemann melting formula [equation (1)] to calculate the Debye temperature once a constant, c′, is evaluated and the melting point temperature known.

The Debye temperature is related to the vibration frequency of atoms in a crystal. The stronger the bond, the greater the Debye temperature and usually the greater the melting point for any series of similar elements. The Debye temperature, θ_D, is usually determined from specific heat or sound velocity measurements. The θ_D obtained from differing methods sometimes yields differing results. In the Lindemann equation the constant c′ can be evaluated by calculating a c′ for each of the rare-earth metals where the Debye temperature, atomic number, and atomic volume are known (15). Table 6 lists the data and the c′ calculated using the Lindemann equation. It can be seen that, for elements with similar structures and bonding, the c′ is very nearly a constant. In averaging the c′ values calculated from the Debye temperature obtained from specific heat measurements (excluding Yb), a value of $\overline{c}'$ = 132 was obtained. Using the melting point determined from the present work, the density measurement of 7.22 g/cm^3 determined by Wheelwright (3) for promethium metal, and the above average value of $\overline{c}'$ = 132, a Debye temperature of 145°K was obtained for promethium metal. In using the value of c′ for neodymium and samarium calculated from the θ_D obtained by the sound velocity measurements, the estimated Debye temperature for promethium is 148°K and 134°K, respectively. The average value of θ_D for promethium is estimated to be 142 ± 13°K.

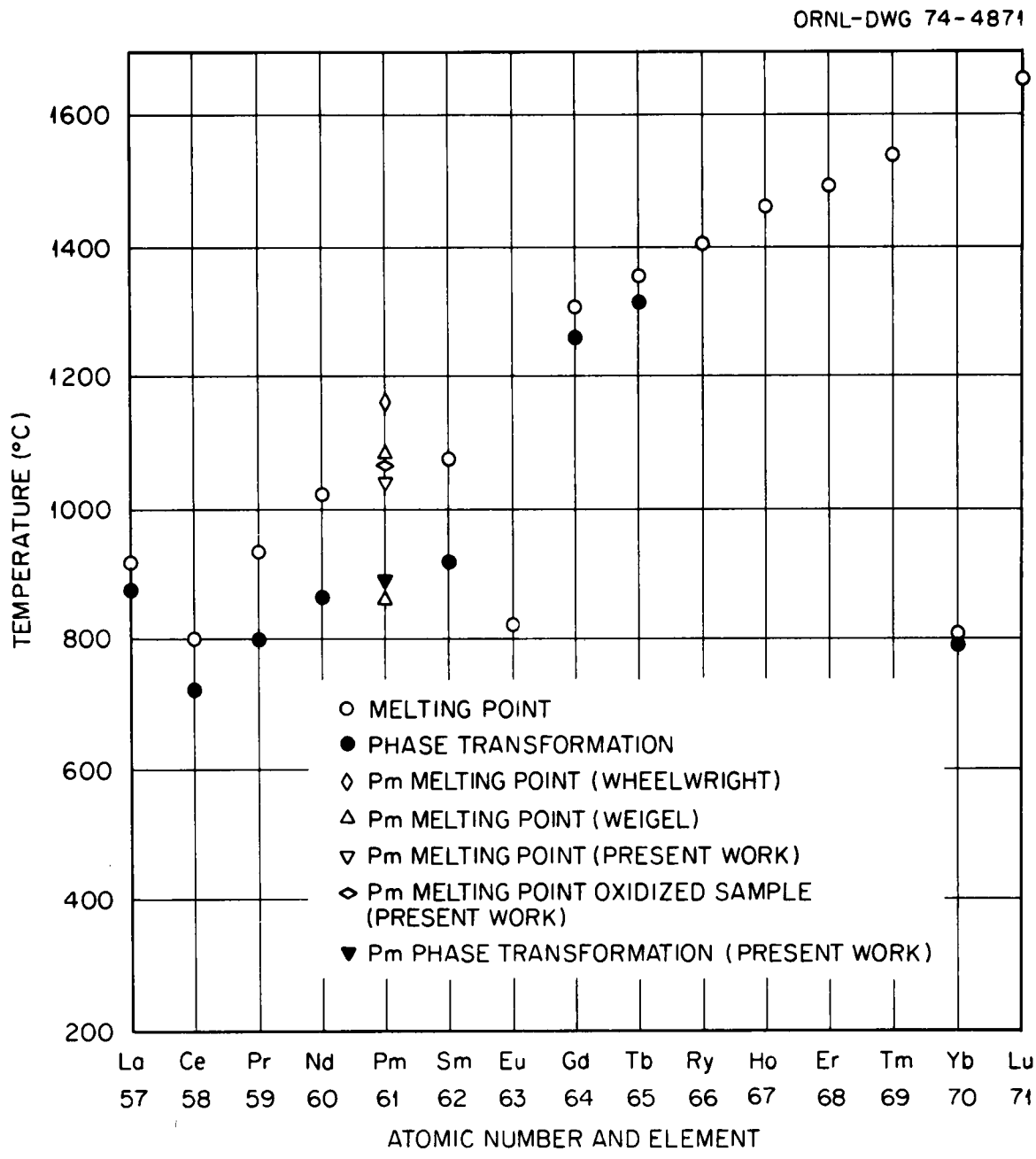


Figure 8. Melting Point and High-Temperature Phase Transformation Data for the Rare-Earth Metals.

Table 6. Debye Temperature Data

Element	Atomic Weight	Atomic Volume	Melting Point (°K)	Specific Heat		Sound	
				Debye Temp (°K)	Constant (c´)	Debye Temp (°K)	Constant (c´)
La	139	22.5	1193	135	130	149	144
Ce	140	21.0	968			135	142
Pr	141	20.8	1208			144	135
Nd	144	20.6	1297			147	134
Pm	147		1315				
Sm	150	19.9	1345	147	133	135	122
Gd	152	19.9	1585	152	128	173	145
Tb	159	19.2	1649	158	131	173	144
Dy	162	19.0	1680	158	131	180	149
Ho	165	18.7	1734	161	132	183	150
Er	167	18.4	1770	163	132	191	155
Tm	169	18.1	1818	167	134		
Yb	173	24.8	1097	94	109	94	109
Lu	175	17.8	1925	166	131		
Y	89	19.8	1782	218	131	250	150

Solid-Solid Phase Transformation

A high-temperature solid-solid phase transformation was found to occur for promethium metal by using the W5Re-W26Re differential thermocouple method. The phase transformation temperature was determined to be 890 ±5°C. This is in the range of values for elements close to promethium (16). The crystal structure of promethium metal is not known; however, from the knowledge of the transformations of the other rare-earth elements, the high-temperature phase for promethium should be bcc (17). The low-temperature phase may be the double hexagonal close-packed structure. In Figure 8 are presented the data for the melting point and high-temperature phase transformation temperatures of the rare-earth elements.

The areas of the DTA curves for the phase transition and the melting point were measured. The area of such curves is proportional to the heat of the transformation, all other factors being constant. The ratio of the two areas from the thermographs yields $\Delta HT/\Delta HF = 0.415$. This value together with other such values where the heat of fusion and heat of transformation (15) have been determined experimentally for other rare-earth elements are presented in Table 7.

Table 7. Heat of Fusion and Heat of High-Temperature Phase Transformation for the Rare-Earth Metals

Element	Heat of Fusion ΔHF (kcal/mole)	Heat of Transformation ΔHT (kcal/mole)	Ratio
Pr	1.650	0.760	0.461
Nd	1.705	0.713	0.417
Pm			0.415[a]
Sm	2.061	0.744	0.360
Gd	2.10	1.03	0.490
Tb	2.20	1.06	0.482

[a]This work.

The value of the ratio for promethium compares very favorably with those for praseodymium and neodymium. It is significantly different than the ratio for samarium. Samarium has a rhombohedral low temperature crystal structure, while praseodymium and neodymium have a double hexagonal close-packed crystal structure. The ratio tends to show that

promethium is similar to praseodymium and neodymium and, therefore, may also have the double hexagonal close-packed structure as its low-temperature crystal structure.

Additional experiments were performed to better understand the problem of relating the DTA areas of the two transformations. Table 8 presents data obtained with silver and gold samples using a similar W5Re-W26Re thermocouple assembly as used in the promethium work. In each of the four cases listed in Table 8 a separate demountable thermocouple was used. One may observe that the areas of the DTA curves decrease for each experiment as to the number of melts or freezes the sample has undergone. This occurs because of vaporization of the sample from the W5Re-W26Re thermocouple. As mass is lost the total heat content affecting the thermocouple decreases, thus the area of the DTA curve diminishes. This effect was noted with silver and gold; it also occurred to some extent in the promethium work. The two thermographs in the ^{147}Pm experiment whose areas were compared were obtained in succession, with the temperature increasing through both transformations and in a time period of less than ten minutes such that the vaporization effect would be minimal.

Another effect is that of the heating or cooling rate through a transformation on the measured DTA area. Noting the results in Table 8, A-1 freeze was performed over a 1-min period. In A-3 and A-5, the temperature was quenched with the cooling rate being at least a factor of 10 greater than in freeze A-1. The values for the DTA areas are not significantly different due to the cooling rates. The differences in areas are due to the vaporization of the sample. Thus, heating or

cooling rate with respect to promethium should not affect the DTA areas significantly. Thus the measured ratio of $\Delta HT/\Delta HF$ for promethium as obtained in these experiments should be an accurate one.

Table 8. Silver and Gold Melting Point Area Determinations

Experiment Number	Melt	Freeze	DTA Area
	Gold, 41.64 mg		
A-1		X	34.10
A-2	X		34.03
A-3		X	32.78
A-4	X		31.61
A-5		X	31.24
	Gold, 80.27 mg		
B-1	X		44.83
B-2		X	41.74
B-3	X		40.32
	Silver, 19.36 mg		
C-1		X	24.64
C-2	X		23.12
C-3		X	28.58
C-4	X		24.38
C-5		X	25.89
	Silver, 59.14 mg		
D-1		X	46.63
D-2	X		38.16
D-3		X	43.51
D-4	X		35.45
D-5		X	41.42
D-6	X		35.21
D-7 (slow)	X		31.00
D-8 (slow)		X	25.65

It was thought that by performing experiments on silver and gold absolute values could be obtained for the heat of fusion and heat of transformation for promethium metal. However, the data in Table 8 show that this method was not useful in determining absolute values of such quantities. A problem encountered was that, in using different demountable thermocouples, different DTA areas would be measured using samples of equal mass for an element. This occurs because of the differences in mass and size of the demountable thermocouple. Such an effect should diminish with a sample of larger mass. Also only those thermographs where the temperature is either increasing or decreasing should be compared, for there was a difference in the areas determined under these two conditions. These are the major problems affecting this method using the present experimental equipment where absolute values for the heat of fusion and the heat of transformation are required.

PART II. VAPOR PRESSURE OF CURIUM-244 METAL

INTRODUCTION

The object of the experiment was to obtain vapor pressure measurements for ^{244}Cm metal. Curium-244 is radioactive and decays by alpha emission to ^{240}Pu. Previous measurements for vapor pressure have been obtained by Smith, Hale, and Thompson (18). The metal had been prepared by reduction of $^{244}CmO_2$ with molten Mg-Zn alloy in the presence of a molten $MgCl_2$-MgF_2 flux at 1050°C as described by Eubanks and Thompson (19). Curium metal has also been prepared by Cunningham and Wallman (20) on a microlevel scale by the reduction of $^{244}CmF_3$ with barium metal. They determined the melting point by the "McWhan" method to be 1340 ± 40°C.

This paper reports the measurement of the vaporization of ^{244}Cm in the temperature range 1270 to 1905°K. The metal had been prepared by reducing $^{244}CmO_2$ with thorium metal in an induction furnace. The ^{244}Cm metal was distilled and collected onto a quartz dome. The vapor pressure results for ^{244}Cm reported in this paper are lower than those reported by Smith *et al.*(18). The crystal structure and lattice parameter for ^{244}Cm metal as reported in this paper are similar to the results obtained by Baybarz and Adair (21) for the high-temperature form of curium metal. The x-ray diffraction results differ with those of Smith *et al.* (18).

VI. THEORY

The Knudsen effusion technique was used to determine the vapor pressure of ^{244}Cm metal. In this method (22) the sample is placed in a container which has a small orifice of known area. The amount of material vaporizing through the orifice in a given period of time is measured. The basic vapor pressure equation is given by

$$P = m(2\pi RT/M)^{1/2} \tag{4}$$

where

P = vapor pressure,

m = rate of mass escape from the orifice,

R = gas constant,

T = absolute temperature, and

M = molecular weight of the vaporizing species.

The above expression can be arrived at by utilizing classical kinetic theory of gases (23). The vapor is assumed to behave as a perfect gas having a velocity distribution f(V).

The total number of molecules which strike a surface per unit time and area is given by

$$N = 1P\bar{v}/4kT \tag{5}$$

where

$\bar{v}$ = average molecular speed,

P = pressure,

k = Boltzmann constant, and

T = absolute temperature.

Experimentally this requires a high vacuum such that the mean free path for molecules is very large with respect to the Knudsen cell and orifice dimensions. Now consider two vacuum regions separated by an infinitely thin wall having a small hole in it. The effusion flow from region 1 to 2 is independent of the effusion flow from region 2 to 1. Once the molecules effuse from region 1, the probability of their returning through the orifice is minimal. Also, if the concentration of the vapor species in region 2 is negligible, the net transfer of the molecular species becomes

$$N_{1\rightarrow 2} = 1P_1\bar{v}/4kT \ . \tag{6}$$

Assuming that the molecules in region 1 have a Maxwellian velocity distribution and that the region and molecules are at one absolute temperature, then the average velocity of a molecule in region 1 becomes

$$\bar{v} = (8RT/\pi M)^{1/2} \tag{7}$$

Converting equation (6) to mass units and substituting equation (7) into equation (6) results in

$$P = m(2\pi RT/M)^{1/2} \tag{8}$$

Thus, temperature uniformity throughout the Knudsen cell is a very important parameter to satisfy experimentally (24).

The rate of mass loss per unit time and per unit area through the orifice can be measured in a variety of ways. In the present experiment, a defined portion of the molecular beam effusing from the orifice was condensed on a collection disc. When the collection disc on which the effusing molecules will condense is of radius R and located coaxially

to the orifice at a distance L, the calculated fraction (25) of the total effusate collected is given by

$$f = R^2/(L^2 + R^2) \ . \qquad (9)$$

In arriving at this result, one must assume a distribution function describing how the molecules effuse from the Knudsen cell orifice. A cosine distribution function was assumed in arriving at the above result. This type of distribution is normally used because of the similarity between this problem and that of black-body radiation from a hole (26). Depending on the experimental conditions, the cosine distribution function may not be the correct one (18, 27).

It is necessary that the molecules in the molecular beam do not undergo any collisions while traversing the distance L. Thus, the vacuum in the region must be high enough such that the mean free path for the molecules is much greater than the distance L. It is also assumed that the condensation coefficient of the effusing molecules on the collection disc is equal to unity. This condensation coefficient relates the number of molecules which condense to the number of molecules which strike the collection disc per unit time. The condensation coefficient can vary depending on the type of molecular beam, the type of material from which the collection disc is made, intensity of the molecular beam, and the temperature of the collection disc.

There are other effects which can influence vapor pressure measurements as determined by this method. Consider the effect of finite sample size and orifice diameter (28). The observed vapor pressure can be related to the equilibrium vapor pressure through equation (10)

$$P_{obs} = P_{eq}/[1 + (a/\alpha A)] \tag{10}$$

where

P_{eq} = equilibrium vapor pressure,

P_{obs} = observed vapor pressure,

a = orifice area,

A = sample area, and

α = sample evaporation and condensation coefficient.

Consider also the effect of the geometry of the orifice region on vapor pressure (29). In the derivation of the ideal Knudsen vapor pressure equation, it was assumed that an orifice was located in an infinitely thin surface. The ratio of effusion flow through a finite geometric hole to that through an infinitely thin membrane is called the Clausing factor W_o. The Clausing factor for the orifice in the Knudsen cell used in the present experiment was calculated to be nearly unity (30).

Alpha counting of the collection discs was performed. In this way, the quantity of ^{244}Cm on the collection disc may be measured. In arriving at a constant relating atomic disintegrations per second to material quantity, a half-life of 18.1 years was used for ^{244}Cm. The quantity of material condensed on the collection discs was corrected for the isotopic purity of curium in the metal.

The final equation for vapor pressure thus becomes

$$P_{eq} = \frac{m_i[1 + (a/\alpha A)]}{[R^2/(L^2 + R^2)]W_o at}\,(2\pi RT/M)^{1/2} \tag{11}$$

where

m_i = mass condensed on the collection disc,

a = orifice area, and

t = time period of experiment.

The Clausius-Clapeyron equation and the perfect gas law may be applied to a metal vapor system in equilibrium (31,32). The result is given in equation (12).

$$\log P = (-\Delta H_T/4.576\ T) + (\Delta S_T/4.576\ T) \qquad (12)$$

where

P = vapor pressure in atmospheres,

ΔH = heat of vaporization,

ΔS = entropy of vaporization, and

T = temperature (°K).

VII. MATERIAL

Initial Cm_2O_3 Material

The curium oxide feed material was batch SRL-31. The isotopic abundance of curium as determined by spark source-mass spectrographic analysis in the oxide is presented in Table 9.

Table 9. Curium Isotopic Content

Curium Mass Number	Isotopic Abundance (atom %)
244	94.26
245	0.880
246	4.74
247	0.077
248	0.042

The impurities as determined by spark source-mass spectrographic analysis on a sample from the SRL-31 oxide are presented in Table 10.

Table 10. Impurities in Batch SRL-31 Curium Oxide

Element	Wt (ppm of Cm)	Element	Wt (ppm of Cm)
Aluminum	20	Lead	100
Calcium	20	Platinum	100
Chromium	100	Silicon	100
Copper	30	Tantalum	150
Iron	1500	Titanium	<100
Potassium	10	Zinc	<20
Manganese	30	Zirconium	<500
Molybdenum	200	Americium	12,000
Sodium	200	Rare Earths	300

The initial feed material contained 88% Cm_2O_3, 8.4% PuO_2, and 1.5% impurities.

The curium metal was prepared by the Target Fabrication Section of the Isotopes Division of ORNL. The metal was prepared by reducing $^{244}CmO_2$ with thorium metal. The tantalum reaction crucible was located in an induction furnace and the ^{244}Cm metal distilled at 2000°C with the metal collected onto a quartz dome. The curium metal was packaged in an argon atmosphere and when received was malleable and grayish in color. The procedure for similarly prepared ^{244}Cm is reported by Baybarz and Adair (21).

VIII. APPARATUS

Vapor Pressure Determination Apparatus

The apparatus consisted of a vacuum furnace (see Figure 2, page 8) and a vapor pressure collection assembly shown in Figure 9. The vapor pressure collection assembly was placed on the top vacuum flange of the furnace bonnet. This positioned the sample collection discs coaxially with the orifice of the Knudsen cell. The base of the collection assembly was fabricated from copper and was cooled by the same chilled water supply that provided cooling to the furnace. Three Viton O-ring vacuum seals were located on the collection assembly. Two were static and one

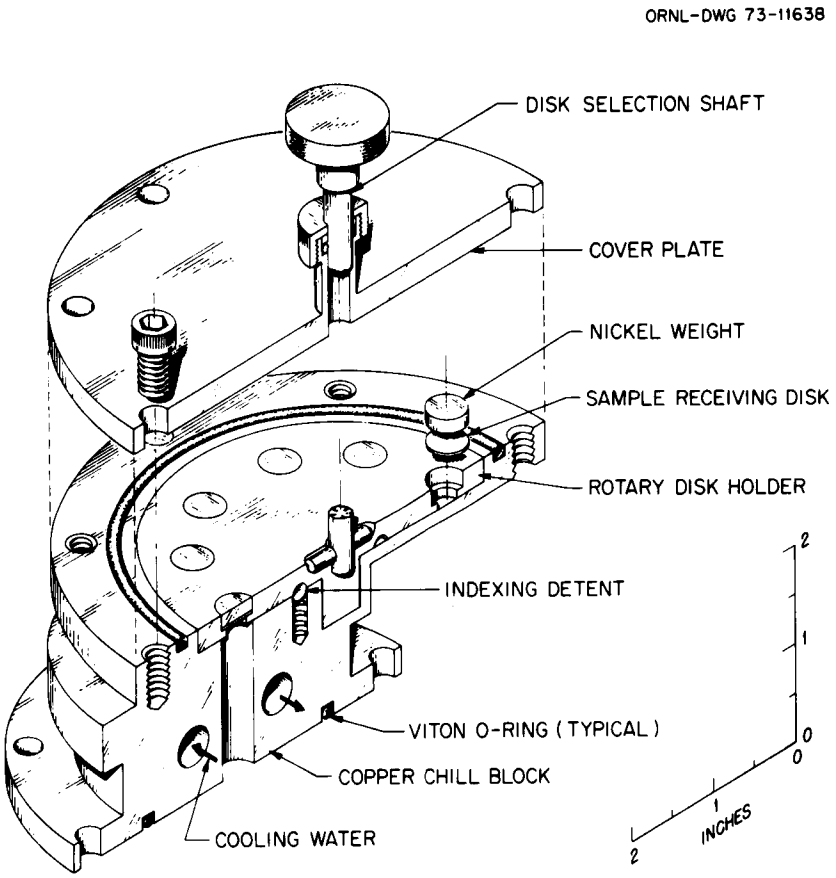


Figure 9. Vapor Pressure Collection Assembly.

was rotary. There were ten spaces available for sample collection discs on the rotor assembly. The rotor was designed with ten off positions such that a sample collection disc need not be exposed during temperature changes and stabilization periods. The sample collection discs were made of platinum metal, 3/8 in. in diameter and 20 mils in thickness. The exposed collection diameter of the discs was 1/4 in. Nickel discs 3/8 in. in diameter and 1/4 in. in height were placed on each sample collection disc. This provided better heat transfer characteristics from the sample collection discs.

A VEECO RG-75 ionization tube was connected to one of the furnace's octal ports and pressure readings were obtained using the tube with a VEECO RG-84 ionization gage located outside the glove box.

The temperature of the Knudsen cell was obtained with a micro-optical pyrometer manufactured by the Pyrometer Instrument Company. The pyrometer was calibrated using National Bureau of Standards bulbs by personnel in the Instrumentation and Controls Division at ORNL. The effects of the furnace window and glove box plate window were taken into account.

The vapor pressure assembly was located in the same glove box in which the promethium metal melting point determination was performed.

X-Ray Diffraction Unit

An x-ray diffraction unit was installed in conjunction with the curium development program (33). The unit used a Norelco vertical goniometer with associated electronics. Two stainless steel alpha handling glove boxes were placed on the main power transformer. The x-ray tube and goniometer section were contained in the main x-ray

process glove box. A Materials Research Corporation vacuum-atmosphere specimen furnace was located on the goniometer section. With this unit, specimens may be heated or cooled or maintained under various types of gases or vacumn. The glove boxes could be purged with argon gas to provide an atmosphere having less than 25 ppm oxygen when handling substances which could otherwise react with air. The unit was installed such that all safety regulations involving alpha handling glove boxes and x-ray diffraction units at ORNL were met. The installation has greatly aided the ability to perform various experiments with radioactive materials.

Knudsen Cell

The Knudsen cell was fabricated from tungsten metal. The diameter of the cell was 5/8 in. and the height measured 3/4 in. The knife-edge orifice diameter was 0.052 in. A black-body hole used for temperature readings was located at the base of the Knudsen cell. Figure 10 shows the Knudsen cell in the heat zone of the furnace.

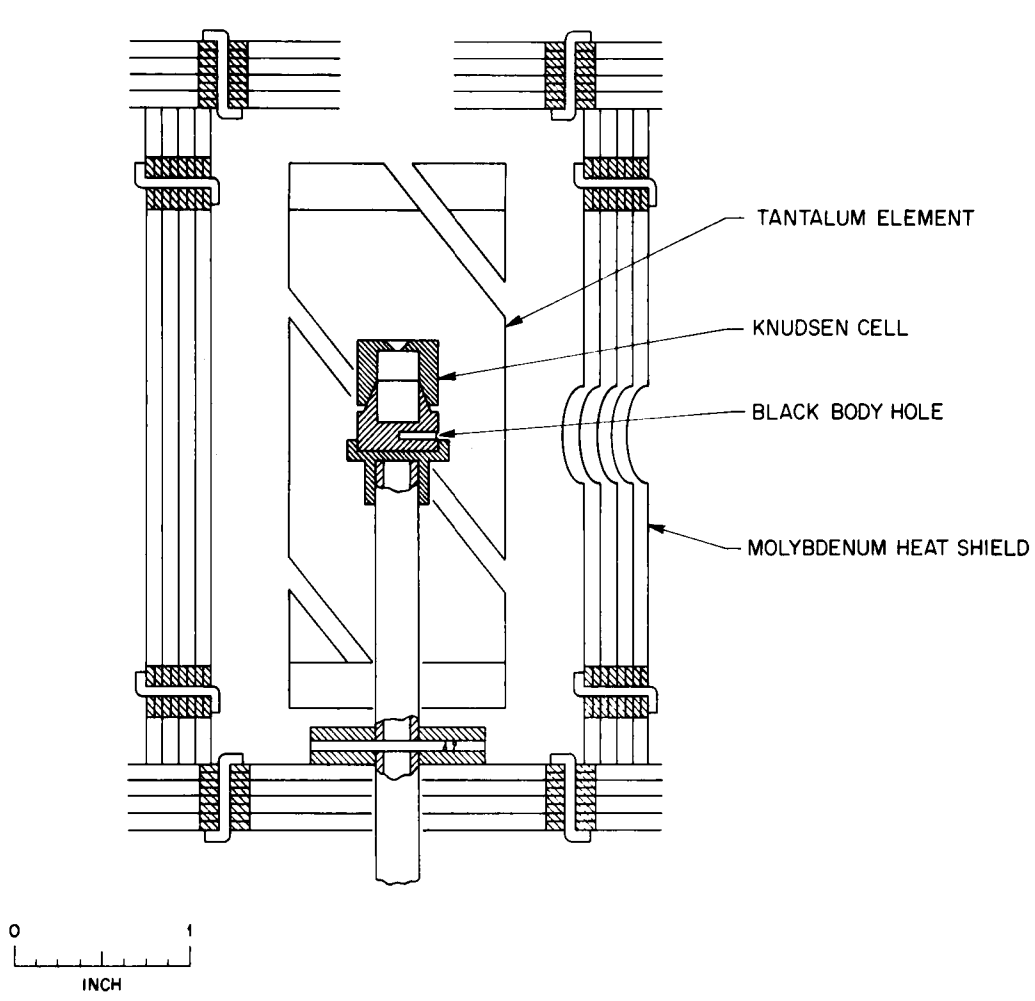


Figure 10. Furnace Heat Zone.

IX. PROCEDURE

Curium Metal Sample Loading

Argon gas was purged into the glove box and the oxygen level was measured using a Beckman G2 oxygen analyzer. When the oxygen level became less than 500 ppm, the curium transfer container was opened and approximately 100 mg of curium metal was loaded into the tungsten Knudsen cell. The Knudsen cell was then loaded into the vacuum furnace, and a vacuum obtained. The argon atmosphere was maintained during progress of the experiment.

Temperature Measurement

During the experiment the black-body hole in the tungsten Knudsen cell could be observed (see Figure 10). The pyrometer temperature readings were recorded and the true temperature was calculated using the calibration data for the pyrometer.

Sample Collection and Measurement

A sample collection disc was exposed for a definite period of time only after the temperature of the Knudsen cell had equilibrated and pressure excursions had ceased. The pressure during these procedures was in the high 10^{-6} torr range as measured by the ionization gage.

At the completion of the eight vapor pressure experiments, the glove box was placed under an argon atmosphere and the rotor assembly was removed from the sample collection assembly. The nickel inserts were removed by using a magnet and placed on a clean surface. Each

sample collection disc was then removed using previously unused and noncontaminated tweezers and placed in their respective uncontaminated sample bottles. Each bottle had previously been identified. The sample bottles were then bagged out of the glove box and the material sent to the General Radioactive Analysis Laboratory section of the Analytical Chemistry Division of ORNL. There each disc was alpha-counted using a high geometry counter and a multichannel analyzer. The average curium alpha counting rate for each sample collection disc was recorded. From the counting rate the amount of ^{244}Cm condensed on each sample collection disc could be determined.

X-Ray Diffraction

The remainder of the curium metal not used in the vapor pressure experiments was transferred to the x-ray diffraction system glove box. The atmosphere in the glove boxes was maintained inert with an argon gas purge. The oxygen level in the glove boxes was less than 25 ppm oxygen. The curium metal was removed from its sealed container and mounted on a Lucite sample holder and the unit placed in the sample zone of the vacuum furnace stage. The furnace was then evacuated, the glove box atmosphere returned to air, and a scan was performed from 10 to 123 degrees 2θ. The unit had previously been calibrated by using a silicon powder specimen.

X. RESULTS

Pyrometer Calibration

The results of the pyrometer calibration and the results of the effects of the furnace window and glove box glass on the temperature measurements are given in Table 11. Data from Table 11 are linearly interpolated and are used in arriving at a resultant true temperature.

Table 11. Optical Pyrometer Calibration

Temperature (°C)				
True	Glass Effect	Pyrometer Calibration	Resultant	Observed
800	-10	37	27	827
1000	-17	20	3	1003
1200	-25	8	-17	1183
1400	-32	10	-22	1378
1400	-32	25[a]	-7[a]	1397
1600	-39	12	-27	1573
1900	-51	10	-41	1859
2200	-70	42	-28	2172

[a]A change in scale on the pyrometer readout device required a change in a built-in red absorption filter.

X-Ray Diffraction

A scan was performed on a curium metal sample from 10 to 123 degrees 2θ. The results are presented in Table 12.

Table 12. X-Ray Diffraction Results of ^{244}Cm Metal

2θ	2θ	Line	a_o
Off chart	Corrected		
30.60	30.699	111	5.040
35.55	35.67	200	5.030
60.99	61.07	311	5.028

The lines which were present were rather broad. This indicates radiation damage in such a crystal. The sample had been maintained at room temperature under a sealed argon atmosphere for approximately one month previous to the scan. The x-ray lines which were present in the scan compare quite well with those obtained by Baybarz and Adair (21). Assigning a face-centered cubic crystal structure to the x-ray diffraction pattern leads to a calculated average lattice parameter of a_o = 5.033 ± 0.003 Å. The data indicate that the vapor pressure experiments were performed on curium metal.

Vapor Pressure

The vapor pressure data of ^{244}Cm metal as determined by the Knudsen effusion technique from 1270 to 1905°K are presented in Table 13. The vapor pressure was calculated using equation (11). The results are given in the order in which the experiments were performed.

Table 13. Vapor Pressure Data

Sample	Temperature Corrected °K	1/T °K	Time at Temp (sec)	Alpha Counts (counts/min)	Pressure (atm)
1	1373	7.283×10^{-4}	3600	5.14×10^{4}	6.637×10^{-10}
2	1680	5.952×10^{-4}	450	1.32×10^{6}	1.466×10^{-7}
3	1270	7.874×10^{-4}	7200	8.61×10^{3}	5.199×10^{-11}
4	1594	6.274×10^{-4}	900	3.49×10^{5}	1.888×10^{-8}
5	1905	5.249×10^{-4}	300	1.57×10^{7}	2.723×10^{-6}
6	1799	5.559×10^{-4}	300	5.51×10^{6}	7.834×10^{-7}
7	1493	6.698×10^{-4}	1800	3.88×10^{6}	8.730×10^{-9}
8	1683	5.942×10^{-4}	900	3.33×10^{5}	2.153×10^{-7}

The vapor pressure and temperature data were fitted to a function of the form of equation (13)

$$Y = A + BX \tag{13}$$

where

$Y = \log_{10}[P(atm)]$

$X = 1/T°K$

A least squares analysis and fit were performed on the data. The Oak-Ridge-Data-Evaluation-And-Analysis-Language statistical computer package was used on the IBM 360 computer. Table 14 presents the calculated coefficients and the standard error of the values. Table 15 presents the input data used in the computer program, the calculated value of the log of the vapor pressure, the deviation, and the standard error of the calculated vapor pressure results. The observed vapor pressure

data and the least squares curve are presented in Figure 11. A weighing factor of 1.0 was used for each experimental point.

Table 14. Coefficients of Fitted Equation

Coefficients	Fitted Value	Standard Error
A	3.831	0.410
B	-17,915	640

Table 15. Statistical Analysis of Vapor Pressure Data

Point	X	Y		Deviation (obs-calc)	Standard Error (calculated)
		Observed	Calculated		
1	7.283×10^{-4}	-9.178	-9.217	3.869×10^{-2}	7.972×10^{-2}
2	5.952×10^{-4}	-6.834	-6.832	-1.853×10^{-3}	5.895×10^{-2}
3	7.874×10^{-4}	-10.284	-10.275	-8.496×10^{-3}	1.108×10^{-2}
4	6.274×10^{-4}	-7.724	-7.409	-3.145×10^{-1}	5.328×10^{-2}
5	5.249×10^{-4}	-5.565	-5.572	-7.686×10^{-3}	8.845×10^{-2}
6	5.559×10^{-4}	-6.106	-6.128	2.206×10^{-2}	7.353×10^{-2}
7	6.698×10^{-4}	-8.059	-8.168	1.096×10^{-1}	5.743×10^{-2}
8	5.942×10^{-4}	-6.667	-6.814	1.472×10^{-1}	5.924×10^{-2}

Using equation (12), equation (13), and the resultant fitted values for A and B presented in Table 14, the heat of vaporization and entropy for curium metal in the temperature range of 1270 to 1905°K are determined to be $\Delta H_T = 82.0 \pm 2.9$ kcal/mole and $\Delta S_T = 17.5 \pm 1.9$ e.u., respectively.

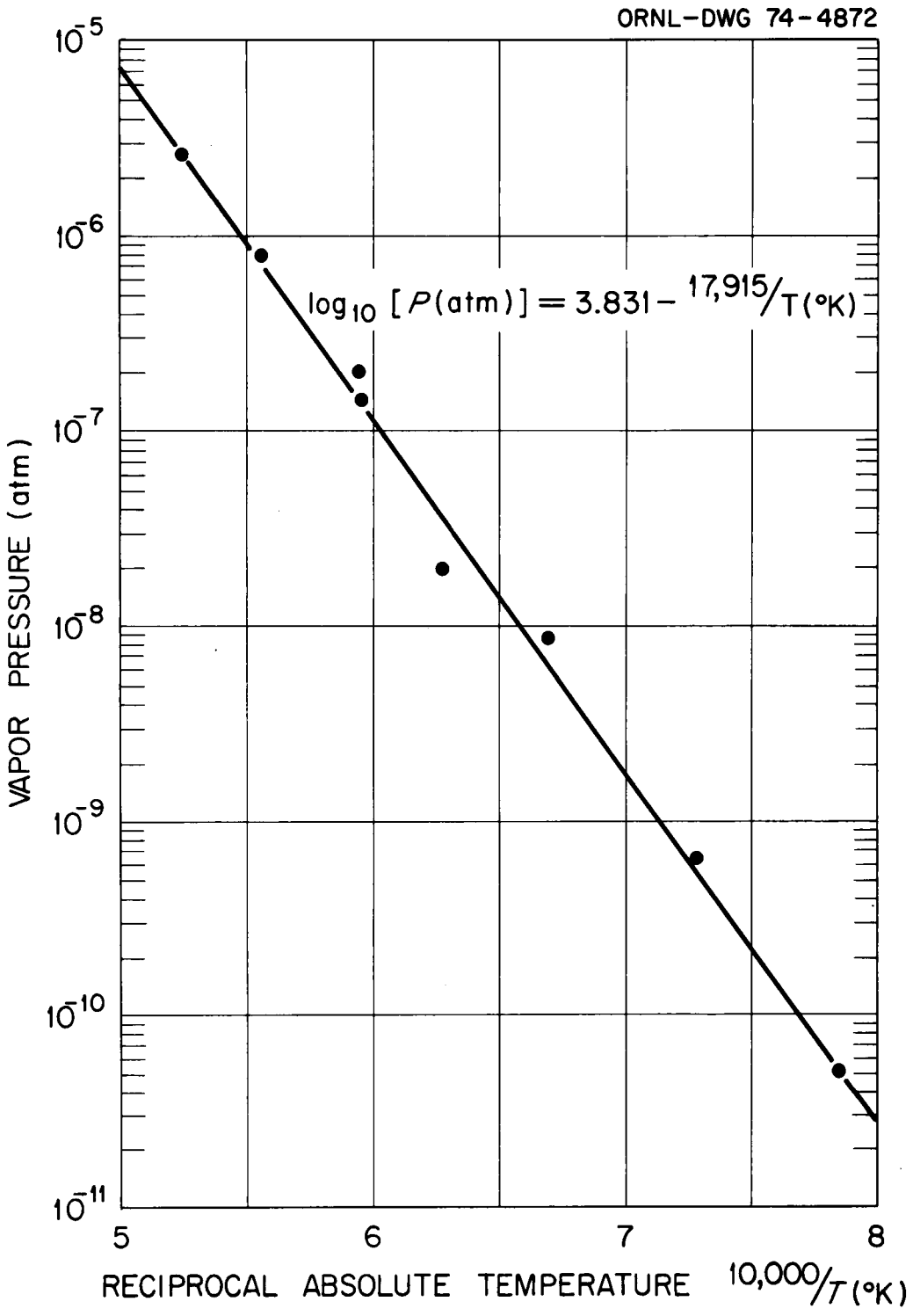


Figure 11. Vapor Pressure of Curium-244 Metal.

XI. DISCUSSION

The determination of the vapor pressure of ^{244}Cm was performed at seven temperatures in the range 1270 to 1905°K. The value for the heat of vaporization and entropy of vaporization in this temperature range was determined to be $\Delta H_{1600°K}$ = 82.0 ± 2.9 kcal/mole and $\Delta S_{1600°K}$ = 17.5 ± 1.9 e.u., respectively. The vapor pressure results reported in the present paper are lower than those reported by Smith, *et al.* (18). The value for $\Delta H_{1600°K}$ and $\Delta S_{1600°K}$ reported by Smith *et al.* (18) are 82.6 ± 2.7 kcal/mole and 21.7 ± 1.7 e.u., respectively. The values for the $\Delta H_{1600°K}$ agree within experimental error. However, the magnitude of the vapor pressures differs by a factor of four. Vapor pressure measurements are very sensitive to temperature. In the experiments by Smith *et al.* (18) the data were correlated using the orifice temperature. The orifice temperature in those cases was lower than the black-body hole measurements at the bottom of the crucible by as much as 17°C. As indicated by Storms (24), the temperature of the sample should be used in most calculations. Storms indicates that the orifice temperature is the significant temperature when the sample has volatilized and collected on the inside surface near the orifice. In the present experiments, the bulk of the sample would not have volatilized and collected on that surface but would have remained near the bottom of the Knudsen cell. The data in the present report are correlated according to the black-body hole temperature at the base of the tungsten Knudsen cell. The majority of the difference in the magnitude of the vapor pressure data of Smith *et al.* (18) and that reported in the present paper can be attributed to the temperature used to correlate the data.

In the present experiment the initial ^{244}Cm metal was analyzed by x-ray diffraction, and the high-temperature structure was measured. The lines were rather broad and weak. This is an indication of a damaged crystal structure due to the alpha decay of ^{244}Cm. A f.c.c. structure was fitted to the lines resulting in a cell parameter value of $a_o = 5.033 \pm 0.003$ Å. This structure and cell parameter compare favorably with the high-temperature crystal structure of ^{244}Cm as determined by Baybarz and Adair (21). An f.c.c. structure of cell parameter $a_o = 5.039$ Å was measured in that case. However, the present result for the cell parameter is different than the high-temperature form of ^{244}Cm determined by Smith *et al.* (18). In that case the residue of a vapor pressure experiment was used in the x-ray analysis. An f.c.c. structure with cell parameter of $a_o = 4.382$ Å was measured.

In the present experiment an x-ray analysis of the sample residue was not performed, for the tungsten Knudsen cell could not be opened. The x-ray diffraction results of the initial ^{244}Cm metal tend to show that vapor pressure experiments were performed on ^{244}Cm metal.

The heat of vaporization at 298°K, $\Delta H_{298°K}$, is used to compare the vaporization behavior of different elements. In order to obtain $\Delta H_{298°K}$ from high-temperature vapor pressure data, one should have experimental values for the heat capacity of the liquid and solid and gaseous phases for the element. One should also have information such as the heat of fusion or heat of transformations, if any transformations occur in the extrapolated temperature range. Such values have not been experimentally determined for ^{244}Cm metal. Thus, $\Delta H_{298°K}$ values for ^{244}Cm will depend on assumed values for the mentioned quantities. It is estimated that

the $\Delta H_{298°K}$ will be approximately 7 kcal/mole greater than the $\Delta H_{1600°K}$ value (34-37). This results when one considers the increase in ΔH_{vap} as determined for elements of the rare-earth and actinide series where experimental values for the needed quantities are available.

LIST OF REFERENCES

LIST OF REFERENCES

1. F. Weigel, *Angew. Chem.* 75, 451 (1963).

2. F. Weigel, *Fifth Rare-Earth Research Conference, Chemistry Session C,* Ames, Iowa, August 30, 1965.

3. E. J. Wheelwright, *J. Phys. Chem.* 73, 2867-71 (1969).

4. Lindemann, *Phys. Zeits.* 11, 609 (1910).

5. J. M. Ziman, *Principles of the Theory of Solids*, Cambridge at the University Press, 1965, Chapters 1 and 2.

6. P. Angelini and H. L. Adair, *Preparation of ^{147}Pm Metal and the Determination of the Melting Point and Phase Transformation Temperatures*, ORNL-TM-4268, Oak Ridge National Laboratory (1974).

7. I. S. Kulikov, *Thermal Dissociation of Chemical Compounds*, translated by J. Schmorak, Israel Program for Scientific Translations, Jerusalem, 1967.

8. R. P. Elliott, *Constitution of Binary Alloys*, First Supplement, McGraw Hill Company, New York, 1965.

9. E. Ryshkewitch, *Oxide Ceramics*, Academic Press, New York, 1960, Chapter 3.

10. E. M. Savitskii, V. F. Terekhova, I. V. Burov, I. A. Markov, and O. P. Naumkin, *Rare Earth Alloys*, Acad. of Science, USSR Moscow, Translation AEC-tr-6151, 1962, Chapter 1.

11. *The Plutonium-Oxygen and Uranium-Plutonium Oxygen Systems: A Thermochemical Assessment*, Technical Report Series No. 79, IAEA, 1967.

12. V. W. Bronger and W. Klemm, *Darstellung von Legierungen des Platins mit unedlen Metallen Zeitschrift für Anorganische und Allgemeine Chemie Band* 319, 58-81, 1962.

13. N. H. Krikorian, "The Reaction of Selected Lanthanide Carbides With Platinum and Iridium," *Journal of the Less Common Metals* 23, 271-79 (1971).

14. P. R. Wengert, *Thermodynamic Stability of Certain Intermetallic Compounds Made From Transition Elements*, UCRL-18727, University of California (1969).

15. K. A. Gschneidner, Jr., *Rare Earth Alloys*, D. Van Nostrand Company, Inc., Princeton, N. J., 1961.

16. F. H. Spedding and A. H. Daane (Eds.), *The Rare Earths*, John Wiley & Sons, Inc., New York, 1961.

17. F. H. Spedding, B. J. Beaudry, J. J. Croat, and P. E. Palmer, *The Preparation and Properties of "Ultrapure" Metals*, IS-2283, UC-25, Ames Laboratory (1970).

18. P. K. Smith, W. H. Hale, and M. C. Thompson, "Vapor Pressure and Crystal Structure of Curium Metal," *J. Chem. Phys.* 50, 5066 (1969).

19. I. D. Eubanks and M. C. Thompson, "Preparation of Curium Metal," *Inorganic Nucl. Chem. Letters* 5 (1969).

20. B. B. Cunningham and J. C. Wallman, *J. Inorg. Nucl. Chem.* 26, 271-75 (1964).

21. R. D. Baybarz and H. L. Adair, "Preparation of the High-Temperature Form of Curium Metal," *J. Inorg. Nucl. Chem.* 34, 3127-30 (1972).

22. M. Knudsen, *Ann. I. Physik* 28, 999 (1909).

23. R. D. Present, *Kinetic Theory of Gases*, McGraw-Hill Book Company, New York, 1958, Chapters 1, 2, and 3.

24. E. K. Storms, *The Effect of an Axial Temperature Gradient on the Apparent Pressure in a Knudsen Effusion Cell*, LADC-6242, CONF-649-1, Los Alamos Scientific Laboratory (1964).

25. A. J. Chapman, *Heat Transfer*, The McMillan Company, New York, 1967, Chapter 11.

26. D. Yakovlevich Svet, *Thermal Radiation*, Consultants Bureau of New York, 1965.

27. R. J. Thorn, *Saturation of Vapor in a Knudsen Effusion Oven*, ANL-5417, Argonne National Laboratory (1955).

28. J. L. Margrave, "Vapor Pressure," p 225-246 in *Physicochemical Measurements at High-Temperature*, ed. by J. O'M Bockris, J. L. White, and J. D. Mackenzie, Butterworths Scientific Publications, 1959.

29. S. Dushman, *Scientific Foundations of Vacuum Technique*, R. H. Lafferty (Ed.), John Wiley & Sons, Inc., 1962, Chapters 1 and 8.

30. R. P. Iczkowski, J. L. Margrave, and S. M. Robinson, "Effusion of Gases Through Conical Orifices," *J. Phys. Chem.* 67, 229 (1963).

31. R. A. Swalin, *Thermodynamics of Solids*, John Wiley & Sons, New York, 1962.

32. F. T. Wall, *Chemical Thermodynamics*, W. H. Freeman and Company, San Francisco, 1958, Chapter 4.

33. H. G. Hunter, R. W. Schaich, and J. A. Setaro, *Safety Analysis of Isotopes Alpha Handling Facility*, ORNL-TM-2845, Addendum No. 2, Oak Ridge National Laboratory (March 1970).

34. D. R. Stull and G. C. Linke, *Thermodynamic Properties of the Elements*, American Chemical Society, 1956.

35. R. J. Ackermann and R. J. Thorn, *The Thermodynamic Behaviour, Thermodynamic Properties and Systematic Trends of Actinide Metal-Oxygen Systems*, Thermodynamic Proceedings Symposium, Vienna, 1965, Vol. 1, pp. 243-269 (1966).

36. F. H. Spedding, A. H. Daane, G. Wakefield, and D. H. Dennison, "Preparation and Properties of High Purity Scandium Metal," *Transactions of the Metallurgical Society of AIME* 218, 608-611 (August 1960).

37. F. H. Spedding, R. J. Barton, and A. H. Daane, "The Vapor Pressure of Thulium Metal," *J. Am. Chem. Soc.* 79, 5160-63 (1957).

VITA

The author was born December 27, 1945, in Mosciano S'Angelo, P. Teramo, Italy. The first son of Joseph and Santarella Angelini. His primary education was received both in Italy and at the St. Patrick School in Weirton, West Virginia. He graduated from Madonna High School in Weirton in May 1963.

He entered West Virginia University in September 1963 and pursued a course of study in Physics being awarded a Bachelor of Science degree in June 1967.

After graduation he was employed by the Union Carbide Corporation at Oak Ridge National Laboratory, Oak Ridge, Tennessee. In September 1967 he enrolled in the graduate program at The University of Tennessee to obtain a Master of Science Degree in Physics.